


Cite this: *RSC Adv.*, 2022, 12, 18333

Pyridine appended 2-hydrazinylthiazole derivatives: design, synthesis, *in vitro* and *in silico* antimycobacterial studies†

Ramkishore Matsa,^a Parameshwar Makam,^{be} Guneswar Sethi,^c
Ahammed Ameen Thottasseri,^{ib} Aswani Raj Kizhakkandiyil,^a Krishna Ramadas,^c
Vignesh Mariappan,^d Agieshkumar Balakrishna Pillai^d and Tharanikkarasu Kannan^{ia}

An array of pyridine appended 2-hydrazinylthiazole derivatives has been synthesized to discover novel chemotherapeutic agents for *Mycobacterium tuberculosis* (*Mtb*). The drug-likeness of pyridine appended 2-hydrazinylthiazole derivatives was validated using the Lipinski and Veber rules. The designed thiazole molecules have been synthesized through Hantzsch thiazole methodologies. The *in vitro* antimycobacterial studies have been conducted using Luciferase reporter phage (LRP) assay. Out of thirty pyridine appended 2-hydrazinylthiazole derivatives, the compounds **2b**, **3b**, **5b**, and **8b** have exhibited good antimycobacterial activity against *Mtb*, an H37Rv strain with the minimum inhibitory concentration in the range of 6.40–7.14 μM . In addition, *in vitro* cytotoxicity of active molecules has been observed against Human Embryonic Kidney Cell lines (HEK293T) using MTT assay. The compounds **3b** and **8b** are nontoxic and their cell viability is 87% and 96.71% respectively. The *in silico* analyses of the pyridine appended 2-hydrazinylthiazole derivatives have been studied to find the mode of binding of the active compounds with KasA protein of *Mtb*. The active compounds showed a strong binding score (–5.27 to –6.23 kcal mol^{–1}).

Received 3rd April 2022

Accepted 3rd June 2022

DOI: 10.1039/d2ra02163c

rsc.li/rsc-advances

1. Introduction

Tuberculosis (TB) is an infectious airborne disease caused by *Mycobacterium tuberculosis* (*Mtb*). TB remained the topmost infectious disease before the coronavirus (COVID-19) pandemic. According to the Global tuberculosis report 2021, there were 9.9 million infections and 1.3 million deaths. The COVID-19 pandemic has halted years of global progress in reducing TB deaths.¹ The majority of existing TB drugs were discovered in the late 1950s, and due to the extensive usage of these drugs for the past seventy years, these drugs are less effective in controlling the disease as *Mycobacterium* has developed resistance to them. Bedaquiline and delamanid are used in conjunction with other TB medicines for curing MDR-

TB.^{2–4} Pretomanid has most recently entered into the market for treating XDR-TB, and it is used in combination with bedaquiline, and linezolid.⁵ Developing new and effective TB drugs for the treatment of XDR-TB and MDR-TB with shorter and simpler regimens with negligible side effects is the need of the hour.

A broad range of established and new scaffolds were tested for their antitubercular activity over the last decade to identify novel anti-TB drugs. Thiazole derivatives are promising compounds to act as antitubercular agents as they are target-specific. Besides, thiazole compounds are known to act as the anticancer,⁶ antitumor,^{7,8} antimalarial,⁹ antimicrobial,¹⁰ anti-inflammatory,¹¹ and anti-hypolipidemic¹² agents. Moreover, the thiazole moiety is structurally analogous to thiolactomycin, an antibiotic that exists naturally but with synthetic challenges.¹³ During the biosynthesis of the *Mtb* cell wall, thiolactomycin inhibits β -ketoacyl-ACP synthase (KasA), leading to the death of *Mtb*.¹⁴ Nitazoxanide (NTZ), a thiazole ring containing oral FDA-approved drug to treat protozoal infections, significantly inhibits intracellular *Mtb* development.^{15,16} Similarly, tizoxanide, a metabolite of NTZ has also been reported to inhibit non-replicative and replicative *Mtb* strains.¹⁷ Interestingly, derivatives of 2-aminothiazole-4-carboxylate are known to be potent inhibitors of *Mtb*'s KasA protein.¹⁸ Due to the wide range of biological activity of 2-amino thiazole derivatives, in our research lab, we synthesized novel and effective 2-amino

^aDepartment of Chemistry, Pondicherry University, Kalapet, Puducherry 605 014, India. E-mail: tharani.che@pondiuni.edu.in

^bDr Param Laboratories, Plot No. 478, BN. Reddy Nagar, Cherlapally, Hyderabad, Telangana 500 051, India

^cCentre for Bioinformatics, Pondicherry University, Puducherry 605 014, India

^dCentral Inter-Disciplinary Research Facility (CIDRF), Sri Balaji Vidyapeeth (Deemed to be University), Puducherry 607 402, India

^eDivision of Research and Innovation, Department of Chemistry, Uttarakhand University, Arcadia Grant, P.O. Chandamwari, Premnagar, Dehradun, Uttarakhand, 248007, India

† Electronic supplementary information (ESI) available. See <https://doi.org/10.1039/d2ra02163c>



thiazole derivatives with antitubercular activity.^{19,20} We found 2-(2-hydrazinyl)thiazole derivatives showed good antitubercular activity when the 2-pyridyl group was introduced at imine carbon of the thiazole ring.²¹ To fine-tune and check the effect of substituents on the antitubercular activity of the derivatives of the pyridine group introduced at the 4th place of the thiazole ring, different functional groups on imine carbon have been incorporated and evaluated in the present investigation for their anti-TB activities. Interestingly, all the pyridine appended 2-hydrazinylthiazole derivatives discussed in the present report show better antitubercular activity than the previously reported derivatives of 2-hydrazinylthiazoles. The detailed results are presented in this paper. The thiazole derivatives discussed in the present investigation have been synthesized easily through classical Hantzsch thiazole methodologies. The advantage of this method is that there is much scope for generating a class of novel thiazole derivatives.²²

2. Results and discussion

2.1. Designing of pyridine appended 2-hydrazinylthiazole through molecular hybridization approach

In the first step of the present investigation, pyridine appended 2-hydrazinylthiazole derivatives have been designed, and molecular hybridization^{23,24} approach was used for this purpose. As given in Fig. 1, the thiazole scaffold is linked to pyridine on one side and the hydrazine group on the other side for better pharmacological properties during the inhibition of TB.

Pyridine is one of the essential heterocyclic scaffolds found in natural substances, such as alkaloids (trigonelline), vitamins (vitamin B3 and B6), coenzymes (nicotinamide adenine dinucleotide), *etc.* Because of its versatile properties, such as water solubility, good chemical stability, and hydrogen bond-forming capability, pyridine moiety plays a vital role in medicinal chemistry. Pyridine derivatives show excellent antitubercular

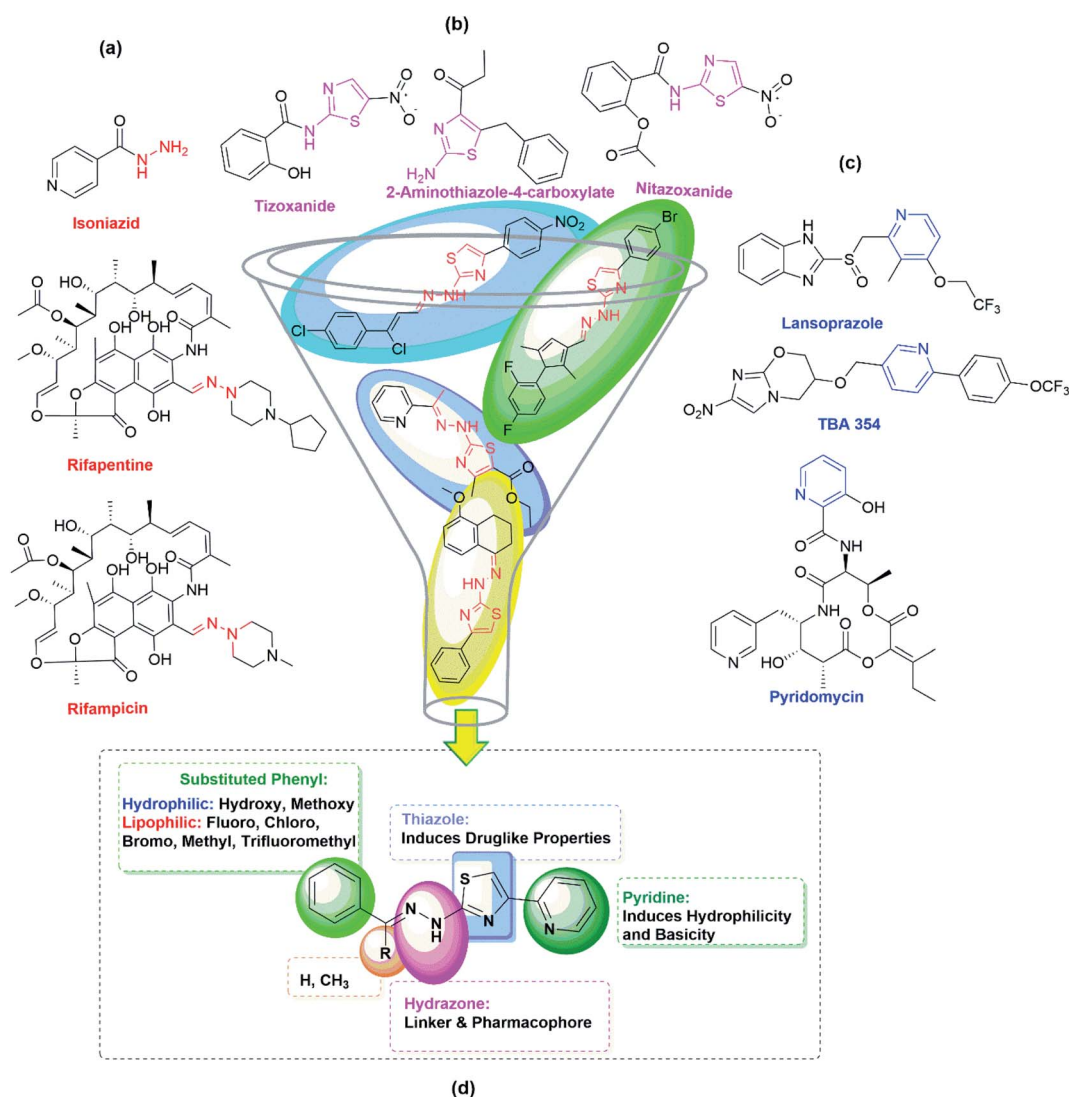


Fig. 1 Design of pyridine appended 2-hydrazinylthiazole by molecular hybridization approach considering the potent antitubercular drugs/agents with (a) hydrazone, (b) 2-aminothiazole and (c) 2-pyridyl derivatives found in the literature, (d) the structure of molecularly hybridized derivatives of pyridine appended 2-hydrazinylthiazoles synthesized in the present investigation.



activity. For example, lansoprazole, a pyridine moiety-containing drug that inhibits gastric acid secretion by binding to the proton-pump receptor, has an intracellular effect against *Mtb*. Lansoprazole kills *Mtb* by attacking the cytochrome bc₁-complex, according to *ex vivo* pharmacokinetic studies.²⁵ Pyridomycin is another pyridine-containing and natural antibiotic drug that demonstrates intense activity against various *Mycobacteria*, including *Mtb* and *M. smegmatis*.²⁶ TBA-354 is another pyridine-containing drug that shows promising antitubercular activity with replicative and static action against *Mtb*.²⁷ The antitubercular activity of pyridine-containing drugs and pyridine-containing derivatives synthesized in our lab previously²¹ prompted us to include a 2-pyridyl scaffold at the 4th place of the thiazole ring in the present investigation. Fig. 1(c) gives the structure of some of the pyridine-containing antitubercular drugs.

The hydrazone ($R_1R_2C=NNH_2$) is another essential and promising scaffold in medicinal chemistry. The lone pair electrons of amine nitrogen are conjugated with the imine group present in hydrazone compounds. The nitrogen atom of the hydrazone is nucleophilic, while the carbon is both electrophilic and nucleophilic.²⁸ These functional features make hydrazone a versatile chemical entity with antimalarial, antiviral, anti-HIV, anti-schistosomiasis, antimicrobial, anthelmintic, anticancer, antiplatelet, antidiabetic, antidepressant, anticonvulsant, anti-inflammatory, analgesic, and antioxidant properties.^{29,30} Moreover, the most promising antitubercular drugs such as rifampicin, isoniazid, and rifapentine contain hydrazone scaffold (see Fig. 1(a)) in their structures. With unique hydrogen bonding donor and receiving regions, hydrazones have gained much attention as potent anti-TB molecules.³¹ The combination of 2-aminothiazole and hydrazone scaffolds in the derivatives of 2-(2-hydrazinyl)thiazole exhibited good inhibitory potentials against the strain of *Mtb*, H37Rv.^{19,32–34} The encouraging results of the *in vitro* studies and the higher possibility of synthesizing different types of substitutions motivated us to synthesize derivatives of pyridine appended 2-hydrazinylthiazole in finding out anti-TB agents with improved inhibitory potentials.

In the second step of this research, Lipinski and Veber rules were used to evaluate the drug-like molecule (DLM) nature of pyridine appended 2-hydrazinylthiazoles.^{35,36} The DLM nature can be found out using molecular weight, log *P* value, number of hydrogen bond acceptors, and donors mentioned in the Lipinski rule. Besides, total polar surface area (TPSA) and the number of rotatable bonds (RBs) mentioned in the Veber rule can also be used to understand the DLM nature of the pyridine appended 2-hydrazinylthiazoles. Molinspiration server has been used to deduce the physicochemical properties of designed pyridine appended 2-hydrazinylthiazoles, and the deduced data are tabulated in Table 1. The results indicate that the molecular weights are in the range of 232.31–370.43, which is less than Lipinski's recommended value of 500. The log *P* values are between 1.64 and 4.10, and these values are less than 5 which is suggested by Lipinski rule. Likewise, the hydrogen bond acceptors of all compounds are between 4 to 7, and hydrogen bond donors are less than two that are far below the

Lipinski rule's recommended values. The total number of RBs of all the compounds is in the range of 4–7, and the TPSA of the compounds is in the range of 50.17–96.00 Å², which is less than the recommended values. Therefore, all these compounds have not violated the Lipinski and Veber rules and have DLM characteristics. The boiled egg diagram of the pyridine appended 2-hydrazinylthiazoles has been predicted through the Swiss ADME web-based tool,³⁷ and the graph is shown in Fig. 2. A compound should have high gastrointestinal absorption to act as an orally active drug (under white region). Most of the pyridine appended 2-hydrazinylthiazoles exhibited high gastrointestinal absorption except compounds **1b** and **2b**, and these compounds have exhibited blood–brain barrier permeation (under yellow region).

2.2. Synthesis of pyridine appended 2-hydrazinylthiazoles

In the third step of this research, as given in Scheme 1, all the designed pyridine appended 2-hydrazinylthiazoles with DLM nature have been synthesized. To synthesize pyridine appended 2-hydrazinylthiazole derivatives, first, thiosemicarbazones were synthesized from thiosemicarbazide and the respective carbonyl compounds using the literature method.^{19,38}

The structure of thiosemicarbazones has been confirmed using different spectroscopic techniques. The characteristic imine proton present in thiosemicarbazones appears as a single peak between 8.5 ppm and 9.0 ppm in the ¹H nuclear magnetic resonance (NMR) spectra, and methyl protons at the imine group resonate between 2.28 ppm to 2.37 ppm. The proton present in –NH resonates between 10.05 ppm and 12.47 ppm, whereas protons present in aromatic groups resonate between 7.00 ppm and 8.4 ppm. In ¹³C NMR spectra, the characteristic imine carbon resonates around 150 ppm, and in the infrared spectra, the stretching vibrations of the characteristic imine group appear in between 1542 and 1579 cm^{–1}. The spectral data of thiosemicarbazones presented here are similar to the already published data.³⁸ In the next step, as shown in Scheme 1, novel pyridine appended 2-hydrazinylthiazole derivatives have been synthesized from 2-(bromoacetyl)pyridine and corresponding thiosemicarbazones using the classical Hantzsch-thiazole synthesis method. All the structures of the novel pyridine appended 2-hydrazinylthiazole derivatives have been confirmed using spectroscopic techniques. The characteristic thiazole proton resonates between 7.5–8.5 ppm, and the methyl protons attached to the imine group resonate around 2–2.5 ppm in ¹H NMR spectra. The –NH protons of thiosemicarbazones resonate at 9.0–9.5 ppm, whereas the same protons resonate downfield at 10.5–12.5 ppm in the derivatives of pyridine appended 2-hydrazinylthiazoles, as a result of aromaticity present in the thiazole ring. The spectral data and spectra of all the novel compounds are given in ESI.† Structures of all the synthesized derivatives of pyridine appended 2-hydrazinylthiazole are given in Table 1.

2.3. Single crystal X-ray studies

In the next step, the single crystals of some of the pyridine appended 2-hydrazinylthiazole derivatives have been grown to



Table 1 Physico-chemical^a, *in vitro* and *in silico* properties of pyridine appended 2-hydrazinylthiazoles^b

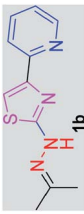
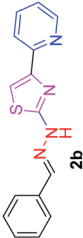
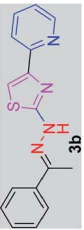
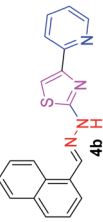
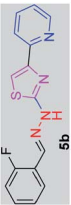
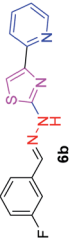
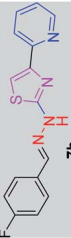
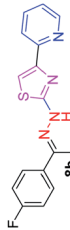
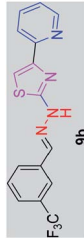
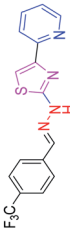
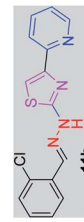
Structure and code	Lipinski rule				Veber rule			<i>In vitro</i>		<i>In silico</i>	
	<i>M_w</i>	log <i>P</i>	HAs	HDs	RBs	TPSA	No. of violations	MIC against <i>Mtb</i> , H37Rv (μM)	Cytotoxicity% against HEK 293t at 6.5 μM	Glide score (kcal mol ⁻¹)	No. of H-bond (interacting residue with distance)
 1b	232.31	2.04	4	1	3	50.17	0	430.46	NA	-5.804	1 (Thr 315, 2.80 Å)
 2b	280.36	2.81	4	1	4	50.17	0	7.13	38.23	-6.233	1 (Thr 315, 2.94 Å)
 3b	294.38	3.26	4	1	4	50.17	0	6.79	87.47	-5.277	1 (Val 278, 3.19 Å)
 4b	330.42	3.97	4	1	4	50.17	0	75.66	NA	-5.015	1 (Thr 315, 2.81 Å)
 5b	298.35	2.93	4	1	4	50.17	0	6.70	41.58	-6.095	2 (Thr 315, 3.29 Å and 2.93 Å)
 6b	298.35	2.95	4	1	4	50.17	0	83.79	NA	-6.165	1 (Thr 315, 2.93 Å)
 7b	298.35	2.98	4	1	4	50.17	0	83.79	NA	-6.186	1 (Thr 315, 2.93 Å)
 8b	312.37	3.42	4	1	4	50.17	0	6.40	92.17	-5.482	1 (Thr 315, 2.90 Å)
 9b	348.35	3.68	4	1	5	50.17	0	71.77	NA	-5.016	2 (Thr 315, 3.25 Å, 2.86 Å)
 10b	348.35	3.71	4	1	5	50.17	0	71.77	NA	-5.039	2 (Thr 315, 3.26 Å, 2.86 Å)
 11b	314.80	3.44	4	1	4	50.17	0	79.42	NA	-5.932	2 (Thr 315, 3.30 Å, 2.81 Å)



Table 1 (Contd.)

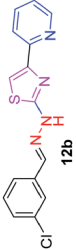
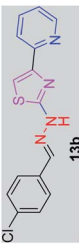
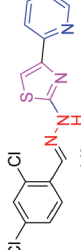
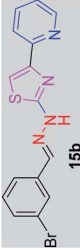
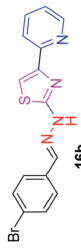
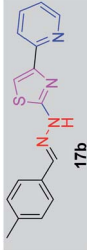
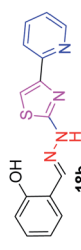
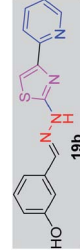
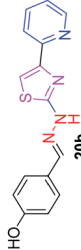
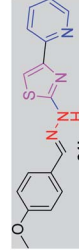
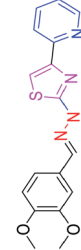
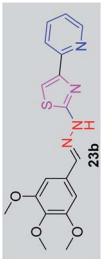
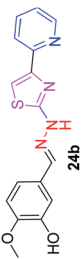
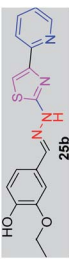
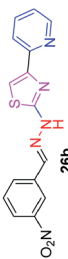
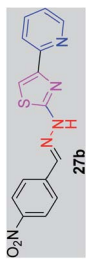
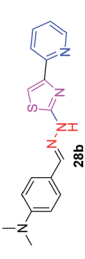
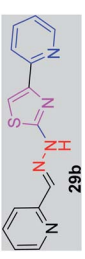
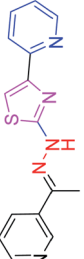
Structure and code	Lipinski rule				Veber rule			<i>In vitro</i>		<i>In silico</i>	
	<i>M_w</i>	log <i>P</i>	HAS	HDs	RBS	TPSA	No. of violations	MIC against <i>Mtb</i> , H37Rv (μM)	Cytotoxicity% against HEK 293t at 6.5 μM	Glide score (kcal mol ⁻¹)	No. of H-bond (interacting residue with distance)
 12b	314.80	3.47	4	1	4	50.17	0	317.66	NA	-6.111	2 (Thr 315, 3.34 Å, 2.95 Å)
 13b	314.80	3.49	4	1	4	50.17	0	79.42	NA	-5.708	2 (Thr 315, 3.28 Å, 2.86 Å)
 14b	349.25	4.10	4	1	4	50.17	0	286.33	NA	-5.932	4 (Thr 315, 3.22 Å, 2.87 Å) (Arg 214, 3.15 Å, 3.25 Å)
 15b	359.25	3.60	4	1	4	50.17	0	278.36	NA	-5.621	1 (Thr 315, 2.80 Å)
 16b	359.25	3.62	4	1	4	50.17	0	278.36	NA	-6.008	2 (Thr 315, 3.22 Å, 2.92 Å)
 17b	294.38	3.26	4	1	4	50.17	0	339.70	NA	-5.035	1 (Thr 315, 2.88 Å)
 18b	296.36	2.75	5	2	4	70.40	0	337.43	NA	-5.707	4 (Thr 315, 3.23 Å, 2.86 Å) (Arg 214, 3.25 Å, 3.19 Å)
 19b	296.36	2.31	5	2	4	70.40	0	337.43	NA	-5.056	2 (Thr 315, 3.21 Å, 2.93 Å)
 20b	296.36	2.33	5	2	4	70.40	0	84.36	NA	-4.685	1 (Thr 315, 3.00 Å)
 21b	310.38	2.87	5	1	5	59.41	0	80.55	NA	-4.949	1 (Thr 315, 2.78 Å)
 22b	340.41	2.46	6	1	6	68.64	0	293.76	NA	-5.019	2 (Thr 315, 3.30 Å, 2.84 Å)



Table 1 (Contd.)

Structure and code	Lipinski rule				Veber rule			In vitro		In silico	
	<i>M_w</i>	log <i>P</i>	HAS	HDS	RBS	TPSA	No. of violations	MIC against <i>Mtb</i> , H37Rv (μM)	Cytotoxicity% against HEK 293t at 6.5 μM	Glide score (kcal mol ⁻¹)	No. of H-bond (interacting residue with distance)
	370.43	2.44	7	1	7	77.88	0	269.96	NA	-4.937	2 (Thr 315, 3.22 Å, 2.86 Å)
	326.38	2.15	6	2	5	79.64	0	306.39	NA	-5.001	2 (Thr 315, 3.21 Å, 2.92 Å)
	340.41	2.53	6	2	6	79.64	0	73.44	NA	-4.985	1 (Thr 315, 2.95 Å)
	325.35	2.75	7	1	5	96.00	0	307.36	NA	-4.517	1 (Met 213, 3.07 Å)
	325.35	2.77	7	1	5	96.00	0	>307.36	NA	-4.87	—
	323.43	2.91	5	1	5	53.41	0	309.19	NA	-4.609	2 (Thr 315, 3.22 Å, 2.91 Å)
	281.34	1.64	5	1	4	63.07	0	355.44	NA	-6.013	2 (Thr 315, 3.29 Å, 2.89 Å)
	295.37	2.02	5	1	4	63.07	0	338.56	NA	-5.640	1 (Thr 315, 2.80 Å)
Rifampicin	—	—	—	—	—	—	—	2.4	NA	NA	NA
Isoniazid	—	—	—	—	—	—	—	NA	NA	-5.830	1 (Thr 315, 2.89 Å)

^a Calculated from molinspiration online server (<https://www.molinspiration.com/cgi-bin/properties>). ^b NA = not analysed.

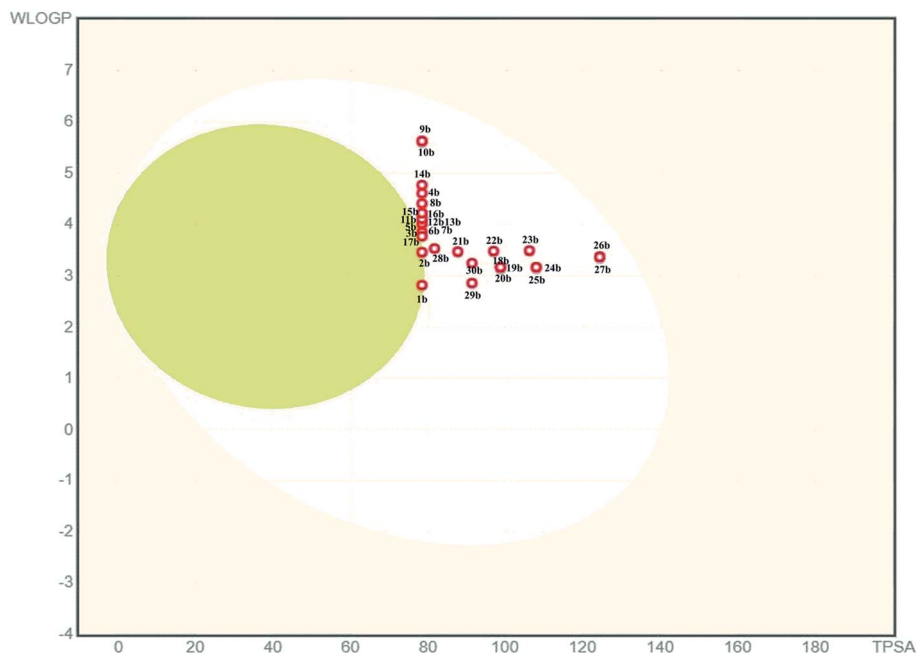
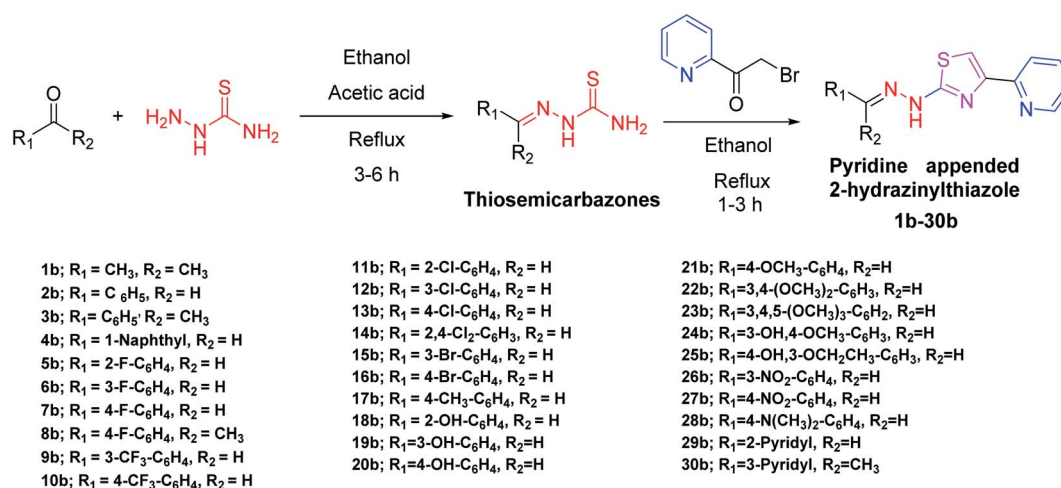


Fig. 2 Boiled egg diagram of pyridine appended 2-hydrazinylthiazoles.



Scheme 1 Synthesis of pyridine appended 2-hydrazinylthiazole derivatives.

understand the crystal packing and spatial orientation. As a representative structure, the crystal packing of a single crystal of **29b** is given in Fig. 3, and the crystal parameters of **29b** are tabulated in Table S1 (see ESI†). The compound **29b** has intermolecular hydrogen bonding with another three molecules of the same compound. The nitrogen atom in a 2-pyridyl ring connected to the imine group forms H-bonding with the N-H group present in another molecule with a distance of 2.197 Å. The N-H group present in the same molecule forms H-bonding with imine substituted 2-pyridyl nitrogen with a distance of 2.063 Å. Likewise, the 2-pyridyl nitrogen, attached to the 4th position of the thiazole ring, interacts with another molecule's N-H group through a hydrogen bonding with a distance of 2.063 Å.

2.4. *In vitro* antitubercular screening of pyridine appended 2-hydrazinylthiazole derivatives

After successful synthesis and characterization, the antitubercular activity of pyridine appended 2-hydrazinylthiazole derivatives have been evaluated against *Mtb*, H37Rv strain using Luciferase reporter phage (LRP) assay. Most of the pyridine appended 2-hydrazinylthiazole derivatives have shown good antitubercular activity than the reported 2-hydrazinyl thiazole derivatives.^{19,39–41} The substitution effect on pyridine appended 2-hydrazinylthiazole derivatives on *Mtb*, H37Rv strain at the imine carbon was evaluated, and results are given in Table 1. The detailed *in vitro* antitubercular activity of pyridine appended 2-hydrazinylthiazole derivatives



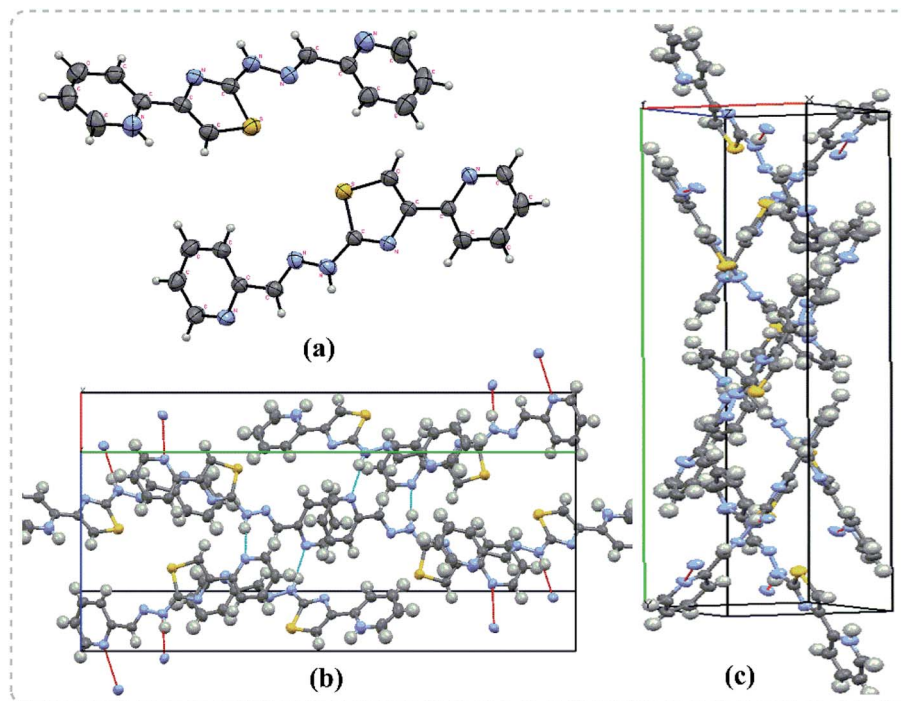


Fig. 3 Single crystal X-ray diffraction results of **29b**. (a) The ORTEP diagram (b) H-bonding interactions (c) double helical shape packing diagram in the crystal lattice.

against *Mtb*, H37Rv are given in Table S2 (see ESI†). The pyridine appended 2-hydrazinylthiazole derivatives are categorized into three groups based on imine carbon substitution. The pyridine appended 2-hydrazinylthiazole derivatives substituted by aliphatic, phenyl, and pyridyl groups are given in one category. The halo and other substituted pyridine appended 2-hydrazinylthiazole derivatives are the other two categories. In the first category, the antitubercular activity of pyridine appended 2-hydrazinylthiazoles substituted with aliphatic, phenyl, and pyridyl groups show the MIC values in the range of 6–431 μM . Among these, phenyl substituted derivatives have shown excellent antitubercular activities. The compound **3b**, phenyl and methyl substitution on the imine carbon of pyridine appended 2-hydrazinylthiazole has shown antitubercular activity with MIC value 6.79 μM . When the methyl group is substituted by the hydrogen in compound **3b**, compound **2b** has shown antitubercular activity with MIC value 7.13 μM . In the case of compound **4b** where the phenyl group is substituted by a naphthyl group in compound **2b**, the antitubercular activity is decreased with the MIC value 75.66 μM . In the case of compounds **30b** and **29b** where pyridyl substitution on the imine carbon of pyridine appended 2-hydrazinylthiazole derivatives have shown insufficient activity with the MIC values 338.56 μM and 355.44 μM , respectively. When two methyl groups are introduced at imine carbon of pyridine appended 2-hydrazinylthiazole, the resulting compound **1b** has shown insufficient antitubercular activity with MIC value 430.46 μM .

In the second category, halogen groups have been introduced on the phenyl ring of the pyridine appended 2-

hydrazinylthiazole derivatives. All these compounds showed antitubercular activity with MIC values in the range of 6–318 μM . When the fluorine atom is substituted on the different positions at the phenyl ring of compound **2b**, the antitubercular activity show MIC values in the range of 6–84 μM . In the case of compound **5b** where fluorine substitution on the 2nd position of the phenyl group present in pyridine appended 2-hydrazinylthiazole, it shows excellent antitubercular activity with the MIC value 6.7 μM . When the fluorine was introduced on third and fourth positions of the phenyl group present in pyridine appended 2-hydrazinylthiazole, the resulting compounds **6b** and **7b** have shown similar antitubercular activity with MIC value 83.79 μM . When the 4-fluorophenyl and a methyl group are substituted at the imine carbon of pyridine appended 2-hydrazinylthiazole, the resulting compound **8b** has shown excellent antitubercular activity with MIC value 6.4 μM . When chlorine atom is introduced on the different positions of phenyl ring of pyridine appended 2-hydrazinylthiazole, the compounds have shown moderate antitubercular activity. In compounds **11b** and **13b**, the chlorine is substituted at second and fourth positions on the phenyl ring of pyridine appended 2-hydrazinylthiazole, and these compounds have shown similar antitubercular activity with MIC value 79.42 μM . When the chlorine atom is substituted at second and fourth positions on the phenyl ring of pyridine appended 2-hydrazinylthiazole, the resulting compound **14b** has shown insufficient antitubercular activity with MIC value 286.33 μM . In the case of compound **12b** where chlorine is substituted at the third position on phenyl ring of pyridine appended 2-hydrazinylthiazole, it has shown



insufficient antitubercular activity with MIC value 317.66 μM . In the case of bromine substitution at third and fourth positions on phenyl ring of pyridine appended 2-hydrazinylthiazoles, the resulting compounds **15b** and **16b** have shown similar antitubercular activity with MIC value of 278.36 μM . When the trifluoromethyl group is introduced at third and fourth positions of phenyl ring of pyridine appended 2-hydrazinylthiazole, the resulting compounds **9b** and **10b** have shown similar antitubercular activity with MIC value 71.77 μM .

In the third category, pyridine appended 2-hydrazinylthiazole derivatives substituted with methyl, methoxy, hydroxy, nitro, and diamine groups on the phenyl ring are considered. The antitubercular activity of these compounds shows the MIC values in the range of 73–340 μM . When a methyl group is substituted at the fourth position on the phenyl ring of pyridine appended 2-hydrazinylthiazole, the resulting compound **17b** has shown insufficient antitubercular activity with MIC value 339.7 μM . When a hydroxy group is substituted at different positions on the phenyl ring of pyridine appended 2-hydrazinylthiazole derivatives, the antitubercular activity was in the range of 84 to 338 μM . In the case of compound **20b** where the 4-hydroxy substituted phenyl ring of pyridine appended 2-hydrazinylthiazole, moderate antitubercular activity was observed with MIC value 84.36 μM . In the case of **18b** and **19b** where –OH group is attached at second and third positions on phenyl ring of pyridine appended 2-hydrazinylthiazole, both the molecules have shown similar antitubercular activity with MIC value 337.43 μM . In the case of compound **21b** where the 4-methoxy group is substituted on the phenyl ring of pyridine appended 2-hydrazinylthiazole, it has shown moderate antitubercular activity with MIC value 80.55 μM . Further increasing the number of methoxy groups on phenyl ring of pyridine appended 2-hydrazinylthiazole, the resulting compounds **22b** and **23b** have shown insufficient antitubercular activity with the MIC values 293.76 μM and 269.96 μM , respectively. In the case of compound **24b** where the –OH group at 3rd position, and methoxy group at the 4th position on the phenyl ring of pyridine appended 2-hydrazinylthiazole insufficient antitubercular activity was observed with MIC value 306.39 μM . When the hydroxy group is substituted at fourth and ethoxy group at third positions on phenyl ring of pyridine appended 2-hydrazinylthiazole, the resulting compound **25b** showed moderate antitubercular activity with MIC value of 73.44 μM . In nitro substitution at third and fourth positions on the phenyl ring, the resulting compounds **26b** and **27b** have shown insufficient antitubercular activity with MIC value 307.36 μM . When the 4-dimethylamine is substituted on the phenyl ring, the resulting compound **28b** has shown poor antitubercular activity with MIC value 309.19 μM . Overall, the compounds **2b**, **3b**, **5b**, and **8b** have shown excellent antitubercular activity with the MIC values range of 6–8 μM . These values are near to the standard rifampicin MIC value, *i.e.*, 2.4 μM . The comparison of MIC values of different pyridine appended 2-hydrazinylthiazole derivatives is shown in Fig. 4.

Similarly, the correlation between log *P* values and their antitubercular activity of pyridine appended 2-

hydrazinylthiazole derivatives is shown in Fig. 5. The log *P* value is gradually increased by introducing lipophilic groups at imine carbon of pyridine appended 2-hydrazinylthiazole. In the first category, the log *P* values of pyridine appended 2-hydrazinylthiazoles are in the range of 1.64 to 3.97, and their MIC values are in the range of 6–431 μM . In the case of pyridyl substituted pyridine appended 2-hydrazinylthiazole derivatives, as in the case of compounds **29b** and **30b**, least log *P* values of 1.64 and 2.02, respectively was observed, and antitubercular activity of these compounds was also poor. When the log *P* value was increased to 2.04, the antitubercular activity decreased for the compound **30b** with the MIC value 430.46 μM . Further, an increase in log *P* value to 3.26 leads to the increased antitubercular activity of the pyridine appended 2-hydrazinylthiazole derivatives. The compounds **2b** and **3b** with the log *P* values 2.81 and 3.26 show good antitubercular activity with MIC values 7.13 μM and 6.79 μM , respectively. When the log *P* value is increased to 3.97, as in compound **4b**, it has shown moderate antitubercular activity with a MIC value of 75.66 μM .

In the second category, the halogen-substituted pyridine appended 2-hydrazinylthiazole derivatives have shown the log *P* value in the range of 2.93–4.1. Compound **5b** has the log *P* value of 2.93 and showed excellent antitubercular activity with a MIC value of 6.7 μM . When the log *P* value is increased to 2.98, the compounds **6b** and **7b** have shown moderate antitubercular activity with MIC value 83.79 μM . Interestingly, a further increase in log *P* to 3.42, compound **8b** has shown excellent antitubercular activity with MIC value 6.4 μM . When the log *P* value is increased to 3.47, the antitubercular activity is decreased for **11b** and **12b** with MIC values 79.42 μM and 317.66 μM , respectively. In the case of compound **13b**, which has the log *P* value of 3.49, it showed moderate antitubercular activity with a MIC value of 79.42 μM . When the log *P* value is increased to 3.62, the compounds **15b** and **16b** have shown similar and inferior antitubercular activity with MIC value 278.36 μM . The compounds **9b** and **10b** have the log *P* values 3.62 and 3.68 and showed similar and moderate antitubercular activity with MIC value 71.77 μM . Further increase in the log *P* value to 4.1, the compound **14b** has shown poor antitubercular activity with MIC value 286.33 μM . In the third category, the pyridine appended 2-hydrazinylthiazole derivatives have log *P* values in the range of 2.15–3.26 and showed moderate to poor antitubercular activity. The compounds **24b** and **19b** have log *P* values 2.15 and 2.31 and showed poor antitubercular activity with MIC values 306.39 μM and 337.43 μM , respectively.

Further increasing the log *P* value to 2.33, the compound **20b** has shown antitubercular activity with MIC value 84.36 μM . When the log *P* value increased to 2.46, the compounds **23b** and **22b** have shown moderate antitubercular activity with MIC values 269.96 μM and 293.76 μM , respectively. Compounds **25b** and **18b** with log *P* values of 2.53 and 2.75 respectively showed antitubercular activity 73.44 μM and 337.43 μM , respectively. When the log *P* value is increased to 2.77, the compounds **26b** and **27b** have shown similar antitubercular activity with MIC value 307.36 μM . Further increasing the log *P* value to 2.87, the compound **21b** has



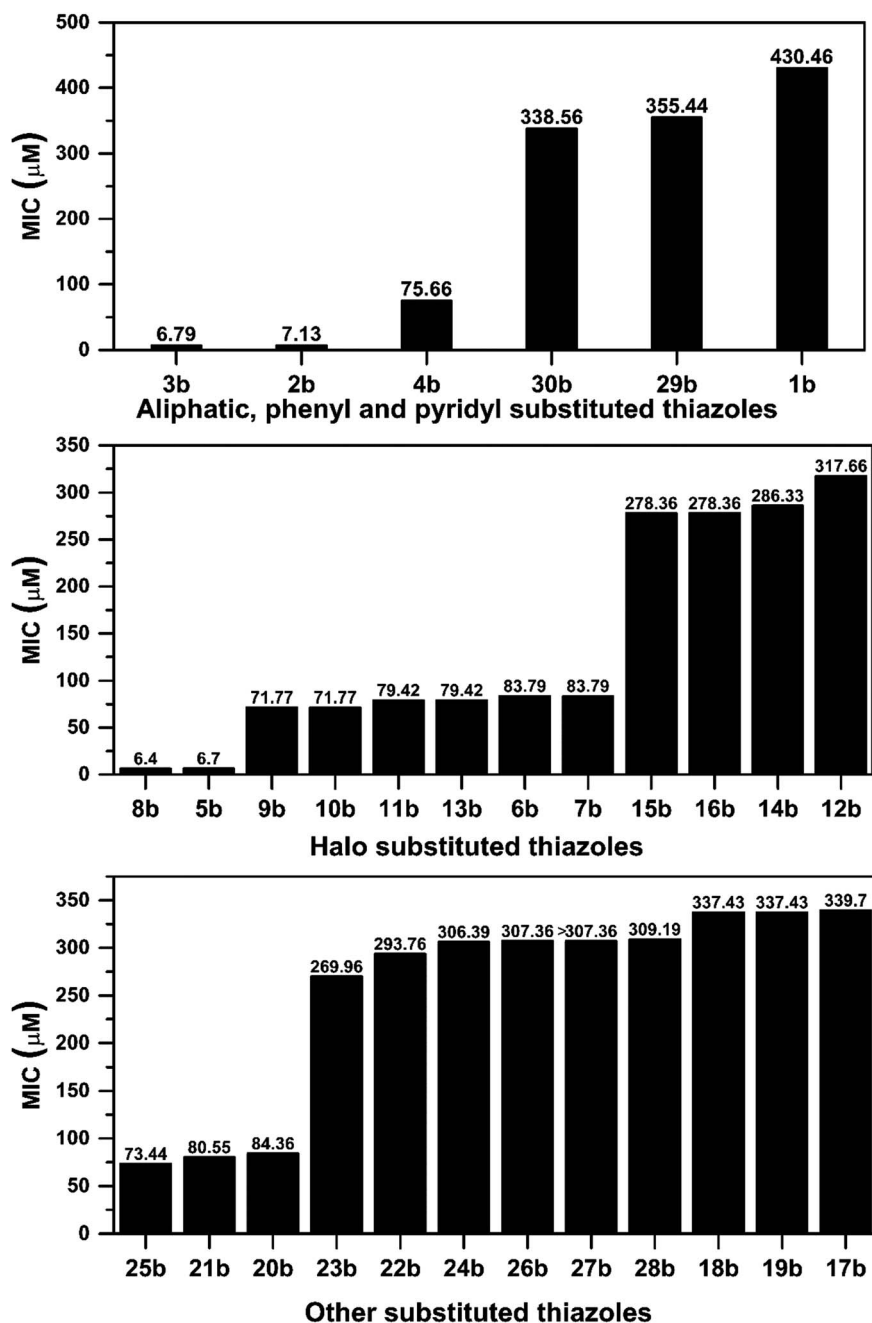


Fig. 4 Correlation between antitubercular activity and substitution on the imine group of pyridine appended 2-hydrazinylthiazoles.

shown moderate antitubercular activity with a MIC value of 80.55 μM. When the log *P* value increased further to 3.26, the antitubercular activity decreased for the compounds 28b and 17b with MIC values 309.19 μM and 339.7 μM, respectively. Overall, most of the active pyridine appended 2-hydrazinylthiazole derivatives have shown good antitubercular activity when the log *P* value in the range of 2.81–3.42.

2.5. *In vitro* cytotoxicity studies of pyridine appended 2-hydrazinylthiazole derivatives

After *in vitro* antitubercular evaluation, the active pyridine appended 2-hydrazinylthiazoles have been tested against

Human Embryonic Kidney Cell lines (HEK 293t) to understand the cytotoxicity of the target thiazole derivatives. The active compounds 2b, 3b, 5b, and 8b were treated with HEK 293t cells at 6.5 μM concentrations, and MTT assay was used to analyse the cell growth. The cell viability of the compounds is in the range of 38–97%, and the results are presented in Fig. 6. Pyridine appended 2-hydrazinylthiazoles have shown more than 50% cell viability considered as nontoxic. The compounds 3b and 8b have shown cell viability at 87.52% and 96.71%, and hence, these compounds are termed to be nontoxic.



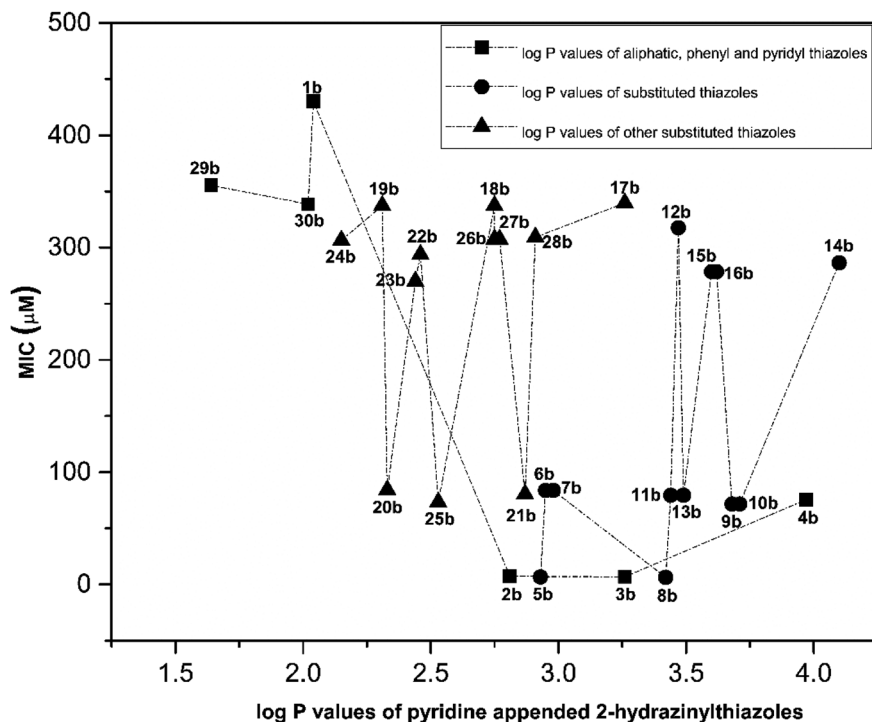


Fig. 5 Correlation between log *P* values of pyridine appended 2-hydrazinylthiazoles and their antitubercular activity.

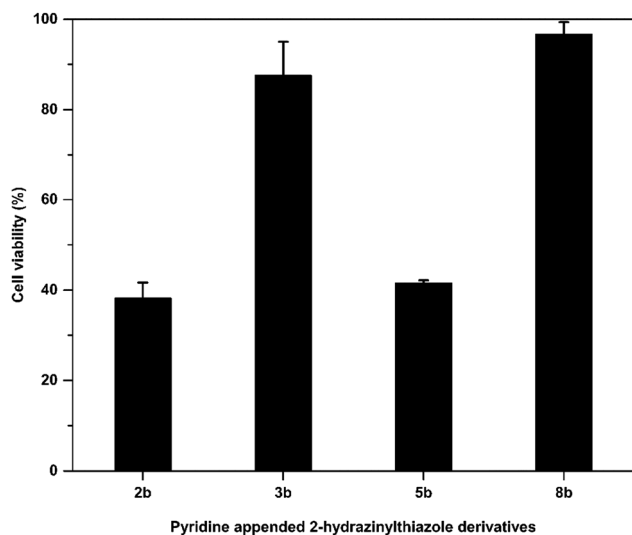


Fig. 6 Cytotoxicity of pyridine appended 2-hydrazinylthiazole derivatives against human embryonic kidney cell lines.

2.6. Molecular docking studies

Docking studies for pyridine appended 2-hydrazinylthiazole derivatives against *Mtb*, KasA protein was carried out in order to determine the mode of action because the 2-aminothiazole pharmacophore is structurally similar to the thiolactomycin (TLM) which is naturally occurring antibiotic.^{13,19} TLM inhibits β -ketoacyl-ACP synthase (KasA) in *mtFabH* fatty acid synthesis, which in turn inhibits cell wall biosynthesis, resulting in *Mtb* death.¹⁴ In the mycolic acid biosynthesis,⁴² the long-chain fatty

acid, KasA protein, plays an important role, thus, KasA protein is selected as a target for docking studies in the present investigation. All the active antitubercular agents have shown good interaction with KasA protein by forming a strong hydrogen bonding with the pyridine appended 2-hydrazinylthiazole molecules. The binding score of the complex was found to be in the range of -4.517 kcal mol⁻¹ to -6.233 kcal mol⁻¹. Some molecules showed a better binding score than standard drug isoniazid, i.e., -5.830 kcal mol⁻¹. The *in silico* results and interaction diagram with *Mtb*, KasA protein are given in Table 1 and Fig. 7, respectively. The hydrophobic interacting residues of the KasA protein of *Mtb* are shown in Table S2 (see ESI†). The active pyridine appended 2-hydrazinylthiazoles have strong interaction with the KasA protein of *Mtb*. The pyridine nitrogen in compound **2b** has hydrogen bonding with Thr 135 residue of KasA protein with a distance of 2.94 Å. This compound has several hydrophobic interactions with Arg 214, Met 213, Ala 215, His 311, Gly 318, Phe 402, Thr 313, Pro 280, Val 278, Phe 404, Ile 317, Ala 279 of KasA protein. In the case of compound **3b**, the hydrazone N–H has hydrogen bonding with KasA protein through Val 278 residue with a distance of 3.19 Å and has several hydrophobic interactions such as Met 213, Arg 214, Ala 215, Ile 317, Ala 279, Pro 280, Thr 313, Thr 315, Gly 318, Asp 319, Glu 322, Phe 402, Gly 403, Phe 404 of KasA protein. The halo substituted active compounds have interaction (s) with Thr 315 residue of KasA protein. Compound **5b** has two hydrogen-bonding interactions with Thr 315. The nitrogen atom in the thiazole ring has one hydrogen bonding with Thr 315 with a distance of 3.29 Å. The nitrogen atom in the pyridine ring has another hydrogen bonding with Thr 315 with a distance of 2.93 Å. Compounds **6b**,



Resolution Magnetic Sector MS DFS mass spectrometer was used to record mass spectra (MS). Rigaku-Oxford Xcalibur Eos single-crystal X-ray diffractometer with Mo-K α radiation ($\lambda = 0.71073$ Å) was used to obtain single crystal X-ray data. For empirical absorption correction, the implemented SCALE3 ABSPACK scaling algorithm was used. The XL in the Olex 2-1.2 package was used for the refinement and SHELXS-97 was used for the structural solution.

4.2. Synthesis of thiosemicarbazone derivatives

Carbonyl compounds (1.1 mmol) and appropriate thiosemicarbazide (1 mmol) were dissolved in ethanol. To this solution, acetic acid (glacial) (a catalytic amount) was added. The resulting solution was refluxed for 3–6 hours and then cooled to room temperature. The resulting precipitate was filtered to obtain the corresponding thiosemicarbazone.

2-(Bromoacetyl)pyridine (1.1 mmol) and appropriate thiosemicarbazone (1.0 mmol) were dissolved in ethyl alcohol. The resulting solution was refluxed for 30 min–6 h and after cooling to room temperature, the reaction mixture was neutralized with an aqueous NaHCO_3 solution. Finally, the solid obtained was filtered and recrystallized from ethyl alcohol to get the final products.

4.4. *In vitro* antimycobacterial assay

4.1. Materials and methods

Bruker Avance-II NMR spectrometer (400 MHz for ^1H nucleus and 101 MHz for ^{13}C nucleus) was used to get NMR spectra. Thermo Nicolet 6700 Fourier transform infrared (FT-IR) spectrometer was used to get FT-IR spectra. Thermo Scientific High-

procedure as follows. About 400 μL of sterile Middlebrook 7H9 broth containing pyridine appended 2-hydrazinylthiazole derivatives at concentrations of $100\text{ }\mu\text{g mL}^{-1}$ were aliquoted into test cryovials (T) and 400 μL of Middlebrook 7H9 broth containing rifampicin ($2\text{ }\mu\text{g mL}^{-1}$) was transferred to drug control cryovial (D). Next, the control cryovial (C) was aliquoted with 400 μL of sterile below-mentioned 7H9 broth (Himedia). *Mtb* H37Rv cell suspension (100 μL) (McFarland no. 2) were used to inoculate all cryovials and incubated at $37\text{ }^{\circ}\text{C}$ for 72 h. Then, 40 μL of 0.1 M CaCl_2 and 50 μL of mycobacteriophage (phAE202) were added into all the cryovials (cell-phage mixture) and incubated for 4 h at $37\text{ }^{\circ}\text{C}$. Then, 100 μL of the cell-phage mixture was transferred to a luminometer cuvette and added with 100 μL of D-luciferin substrate (Cayman chemicals, USA). The relative light unit (RLU) was measured at 10 s integration time in a luminometer (Lumat 9508, Berthold, Germany). The compounds considered as an antitubercular agent if test compounds showed a 50% reduction in RLU when compared to the control RLU. The % of RLU reduction was calculated by using the below-mentioned formula.

$$\text{RLU reduction (\%)} = \frac{\text{control RLU} - \text{test RLU}}{\text{control RLU}} \times 100$$

The active compounds were further tested for their antitubercular activities at $25\text{ }\mu\text{g mL}^{-1}$ and $2\text{ }\mu\text{g mL}^{-1}$ concentrations by LRP assay, as mentioned above.

4.5. *In vitro* cytotoxicity assay

4.5.1. Cell culture. The human embryonic kidney cells (HEK 293T) were maintained at $37\text{ }^{\circ}\text{C}$ under 5% CO_2 and 100% humidity in Dulbecco's modified eagle media and supplemented with 10% fetal bovine serum and antibiotics (200 $\mu\text{L mL}^{-1}$ penicillin G, 200 $\mu\text{g mL}^{-1}$ streptomycin). When the cells reached confluence, they were trypsinized and plated in 96 well culture plates at a concentration of 1×10^4 cells per well, and incubated for 24 h at $37\text{ }^{\circ}\text{C}$ under 5% CO_2 to obtain a monolayer culture. The cells were treated with four pyridine appended 2-hydrazinylthiazole derivatives at $6.5\text{ }\mu\text{M}$ concentration. Cells with no drug treatment and only with DMSO were maintained as control. The experiments were carried out in triplicate. Following a 24 h incubation period at $37\text{ }^{\circ}\text{C}$ under 5% CO_2 , the cell viability was assessed.

4.5.2. MTT assay. The media was aspirated from each well of the culture plate. First, 20 μL of MTT reagent (5 mg mL^{-1}) was added and incubated for 4 h at $37\text{ }^{\circ}\text{C}$ in the CO_2 incubator, and then added 180 μL of dimethyl sulphoxide. Next, the formation of purple crystal formazan was solubilized by placing the plates on a shaker. Then, at a wavelength of 570 nm, the absorbance was measured using a microplate reader. By calculating (absorbance of treated cells/absorbance of untreated cells) \times 100, the percentage of cell viability was calculated.

4.6. Molecular docking

To perform the molecular docking study, the protein was retrieved from the RCSB protein data bank ([https://](https://www.rcsb.org/pdb/home/home.do)

www.rcsb.org/pdb/home/home.do). Before the docking study, the target protein was prepared using the protein preparation wizard, in which the protein was pre-processed, optimized, and minimized. Similarly, to prepare the ligands for docking in maestro format, Schrodinger v11.5 (LigPrep module) was used. A grid box was generated around the protein in which the ligands bind to the protein's active site. The prepared protein and ligands were docked using Schrodinger v11.5. The glide score was calculated within the Schrodinger v11.5 software. The active site prediction was made using the COACH server,⁴⁴ which can be accessed freely. The COACH server is generally used to predict protein-ligand binding sites. The LIGPLOT (version 4.5.3) program was used to generate schematic representations of protein-ligand complexes. UCSF Chimera (version 1.5.3) has been used for 3-D visualization and structural analysis of protein-ligand complex.

Conflicts of interest

There are no conflicts to declare.

Acknowledgements

We are grateful to Mr Anbarasu Sivaraj, Sathyabama Institute of Science and Technology, Chennai, India for the generation of the antitubercular data against *Mtb*, H₃₇Rv strain. University Research Fellowship (URF) to Mr Ramkishore Matsa by Pondicherry University is gratefully acknowledged. Funding by University Grants Commission (UGC), New Delhi (No. F.540/6/DSA-1/2016/(SAP-1) dated 31-10-2018) to Department of Chemistry, Pondicherry University is gratefully acknowledged. We acknowledge Pondicherry University's Central Instrumentation Facility (CIF) for their support in characterizing pyridine appended 2-hydrazinylthiazole derivatives.

References

- 1 World Health Organization, *Global Tuberculosis Report 2021*, 2021.
- 2 C. R. Horsburgh, C. E. Barry and C. Lange, *N. Engl. J. Med.*, 2015, **373**, 2149–2160.
- 3 L. G. Dover and G. D. Coxon, *J. Med. Chem.*, 2011, **54**, 6157–6165.
- 4 B. Liu, F. Li, T. Zhou, X.-Q. Tang and G.-W. Hu, *J. Heterocycl. Chem.*, 2018, **55**, 1863–1873.
- 5 S. J. Keam, *Drugs*, 2019, **79**, 1797–1803.
- 6 E. L. Luzina and A. V. Popov, *Eur. J. Med. Chem.*, 2009, **44**, 4944–4953.
- 7 S. M. El-Messery, G. S. Hassan, F. A. M. Al-Omary and H. I. El-Subbagh, *Eur. J. Med. Chem.*, 2012, **54**, 615–625.
- 8 J. Cai, M. Sun, X. Wu, J. Chen, P. Wang, X. Zong and M. Ji, *Eur. J. Med. Chem.*, 2013, **63**, 702–712.
- 9 P. Makam, P. K. Thakur and T. Kannan, *Eur. J. Pharm. Sci.*, 2014, **52**, 138–145.
- 10 R. P. Karuvalam, K. R. Haridas, S. K. Nayak, T. N. Guru Row, P. Rajeeesh, R. Rishikesan and N. S. Kumari, *Eur. J. Med. Chem.*, 2012, **49**, 172–182.



- 11 M. H. M. Helal, M. A. Salem, M. S. A. El-Gaby and M. Aljahdali, *Eur. J. Med. Chem.*, 2013, **65**, 517–526.
- 12 S. N. Mokale, P. T. Sanap and D. B. Shinde, *Eur. J. Med. Chem.*, 2010, **45**, 3096–3100.
- 13 G. Pappenberger, T. Schulz-Gasch, E. Kuszniir, F. Müller and M. Hennig, *Acta Crystallogr., Sect. D: Biol. Crystallogr.*, 2007, **63**, 1208–1216.
- 14 S. R. Luckner, C. A. Machutta, P. J. Tonge and C. Kisker, *Structure*, 2009, **17**, 1004–1013.
- 15 S. Ranjbar, V. Haridas, A. Nambu, L. D. Jasenosky, S. Sadhukhan, T. S. Ebert, V. Hornung, G. H. Cassell, J. V Falvo and A. E. Goldfeld, *iScience*, 2019, **22**, 299–313.
- 16 L. M. Fox and L. D. Saravolatz, *Clin. Infect. Dis.*, 2005, **40**, 1173–1180.
- 17 E. P. Haraus, K. A. Chervenak, C. E. Good, M. R. Jacobs, R. S. Wallis, M. Sanchez-Felix and W. H. Boom, *Tuberculosis*, 2016, **98**, 92–96.
- 18 Q. Al-Balas, N. G. Anthony, B. Al-Jaidi, A. Alnimr, G. Abbott, A. K. Brown, R. C. Taylor, G. S. Besra, T. D. McHugh, S. H. Gillespie, B. F. Johnston, S. P. Mackay and G. D. Coxon, *PLoS One*, 2009, **4**, e5617.
- 19 P. Makam, R. Kankanala, A. Prakash and T. Kannan, *Eur. J. Med. Chem.*, 2013, **69**, 564–576.
- 20 P. Makam and T. Kannan, *Eur. J. Med. Chem.*, 2014, **87**, 643–656.
- 21 P. Makam, R. Kankanala, A. Prakash and T. Kannan, *Eur. J. Med. Chem.*, 2013, **69**, 564–576.
- 22 M. A. Metwally, E. Abdel-Latif, F. A. Amer and G. Kaupp, *J. Sulfur Chem.*, 2004, **25**, 63–85.
- 23 C. Viegas-Junior, A. Danuello, V. D. S. Bolzani, E. J. Barreiro and C. A. M. Fraga, *Curr. Med. Chem.*, 2007, **14**, 1829–1852.
- 24 C. A. M. Fraga, *Expert Opin. Drug Discovery*, 2009, **4**, 605–609.
- 25 J. Rybníček, A. Vocat, C. Sala, P. Busso, F. Pojer, A. Benjak and S. T. Cole, *Nat. Commun.*, 2015, **6**, 7659.
- 26 R. C. Hartkoorn, C. Sala, J. Neres, F. Pojer, S. Magnet, R. Mukherjee, S. Uplekar, S. Boy-Röttger, K.-H. Altmann and S. T. Cole, *EMBO Mol. Med.*, 2012, **4**, 1032–1042.
- 27 S. Ntshangase, A. Shobo, H. G. Kruger, A. Asperger, D. Niemeyer, P. I. Arvidsson, T. Govender and S. Baijnath, *Xenobiotica*, 2018, **48**, 938–944.
- 28 E. J. Corey and D. Enders, *Tetrahedron Lett.*, 1976, **17**, 11–14.
- 29 S. Rollas and G. S. Küçükgül, *Molecules*, 2007, **12**.
- 30 Ł. Popiołek, *Med. Chem. Res.*, 2017, **26**, 287–301.
- 31 B. Mathew, J. Suresh, M. J. Ahsan, G. E. Mathew, D. Usman, P. N. S. Subramanyan, K. F. Safna and S. Maddela, *Infect. Disord.: Drug Targets*, 2015, **15**, 76–88.
- 32 P. Makam, P. K. Thakur and T. Kannan, *Eur. J. Pharm. Sci.*, 2014, **52**, 138–145.
- 33 A. Arshad, H. Osman, M. C. Bagley, C. K. Lam, S. Mohamad and A. S. M. Zahariluddin, *Eur. J. Med. Chem.*, 2011, **46**, 3788–3794.
- 34 G. Turan-Zitouni, Z. A. Kaplancıklı and A. Özdemir, *Eur. J. Med. Chem.*, 2010, **45**, 2085–2088.
- 35 C. A. Lipinski, *Drug Discovery Today: Technol.*, 2004, **1**, 337–341.
- 36 D. F. Veber, S. R. Johnson, H. Y. Cheng, B. R. Smith, K. W. Ward and K. D. Kopple, *J. Med. Chem.*, 2002, **45**, 2615–2623.
- 37 A. Daina, O. Michielin and V. Zoete, *Sci. Rep.*, 2017, **7**, 42717.
- 38 R. Matsa, P. Makam, M. Kaushik, S. L. Hoti and T. Kannan, *Eur. J. Pharm. Sci.*, 2019, 104986.
- 39 K. K. Roy, S. Singh, S. K. Sharma, R. Srivastava, V. Chaturvedi and A. K. Saxena, *Bioorg. Med. Chem. Lett.*, 2011, **21**, 5589–5593.
- 40 P. V. Sowmya, B. Poojary, V. Kumar, U. Vishwanatha and P. Shetty, *Arch. Pharmacol. Res.*, 2017, DOI: [10.1007/s12272-017-0967-1](https://doi.org/10.1007/s12272-017-0967-1).
- 41 M. Hublikar, V. Kadu, J. K. Dublad, D. Raut, S. Shirame, P. Makam and R. Bhosale, *Arch. Pharm.*, 2020, **353**, 2000003.
- 42 R. Veyron-Churlet, S. Bigot, O. Guerrini, S. Verdoux, W. Malaga, M. Daffé and D. Zerbib, *J. Mol. Biol.*, 2005, **353**, 847–858.
- 43 A. Sivaraj, V. Kumar, R. Sunder, K. Parthasarathy and G. Kasivelu, *J. Cluster Sci.*, 2020, (31), 287–291.
- 44 J. Yang, A. Roy and Y. Zhang, *Bioinformatics*, 2013, **29**, 2588–2595.

